Propagation of Guided Waves in Coated Tubes used in Off-Shore Oil Industry

Kelly Robert-Svendsen Rassier, Boris N. Rojo Tanzi, Guilherme S. da Silva, Mario R. Sobczyk, Ignacio Iturrioz

Department of Mechanical Engineering, Federal University of Rio Grande do Sul (UFRGS)
R. Sarmento Leite 425, 90050-170, Porto Alegre/RS, Brazil
boris.rojotanzi@ufrgs.br

Abstract. This work applies acoustic emission methods to monitor pipes' integrity and mechanical behavior in the offshore oil industry, which cannot be inspected visually because they are usually covered with a polymeric layer to mitigate impact loadings. The elastodynamic response of such a pipe is studied through dispersion curve charts, implemented with commercial finite element packages: one based on the modal analysis of an axisymmetric model, and the other using periodic boundary conditions over a 3D model. Both curves are compared to analytical models based on the classical theories of beam-shaft-bar structures, with effective properties obtained by Voigt theory, leading to an in-depth discussion about the corresponding mechanical behavior of the overall structure.

Keywords: Guided Waves, Off-Shore pipes, Dispersion Curves, Elastodynamic Behavior.

1 Introduction

Oil and natural gas are ubiquitously used non-renewable natural resources extracted from ever-increasing operational depths under the sea. Therefore, its exploitation is also increasingly challenging in several aspects, such as ensuring the integrity of its pipelines. Present-day pipelines are of the rigid multilayer pipe, made of composite structures with metal and polymer layers for different purposes. The function of the outer polymeric layers is to preserve the temperature of the fluid flow, thus preventing the formation of hydrocarbon precipitates and pressure loss [1]. They also protect the pipeline from accidental impacts and prevent the appearance and propagation of collapse waves, a typical phenomenon in these structures. The main steel layer, in turn, provides resistance against the high pressures of the seawater, which is the primary stress source for these pipelines, and one of the critical scenarios in this context is the propagation of buckling waves when a localized defect causes the pipe to fail under external pressure levels that are lower than that for collapse.

Monitoring the integrity or mechanical properties of structures using wave propagation is a classic theme in nondestructive testing (NDT) methods, widely used in engineering applications such as the petrochemical [2, 3] and rail [4, 5] industries. Guided waves occur in geometries where dimensions are predominant in specific directions, as in plates and pipes. When waves propagate through the latter, the width and thickness dimensions are much smaller than the axial one, causing internal reflections and refractions due to interactions with the body's boundaries. As a result, propagation modes are formed throughout the pipe. Comparing these modes in the actual structure with their theoretical prediction provides valuable information about the structure's elastodynamic behavior. Since guided waves can propagate for tens of meters and are a financially viable means of inspection, they are an attractive option for monitoring the integrity of pipes in great depths, a difficult task to perform through other measurement techniques.

2 Theoretical foundation

According to Rose [6], the propagation medium is said to be infinite when the wavelength (L_λ) is much smaller than the dimensions of the cross-section of the body through which this wave passes, or in the ideal case when the body is unbounded. Under these conditions, mechanical waves can be split into two kinds, the longi-

tudinal waves (P waves) and transverse waves (S waves), which travel at constant speeds c_1 and c_2, respectively. Equation (1) and eq. (2) respectively determine these propagation velocities, where λ and μ are the so-called Lamé parameters for the material.

$$c_1 = \sqrt{\frac{\lambda + 2\mu}{\rho}} \tag{1}$$

$$c_2 = \sqrt{\frac{\mu}{\rho}} \tag{2}$$

When the propagation medium is not infinite, the waves interact with the material surfaces, generating linear combinations of modal waves P and S whose characteristics are directly linked to the analyzed geometry. When the medium is semi-infinite (i.e., it has only one free surface), the interaction between P and S waves at and near-below the free surface induces other types of waves, the most important being the Rayleigh one. If the dimensions of the medium are finite, the reflection and refraction of waves affect the propagation, and the medium becomes dispersive. When at least one dimension of a body can be regarded as infinite, it is called a waveguide, with predictable propagation properties that depend on the geometric shape and the wave's frequency and wavenumber. The relationship between the wave and the medium's geometry ends up generating a phenomenon known as dispersion, which is the variation of propagation speed as a function of frequency [6]. This phenomenon is the basis for using guided waves as a nondestructive testing method, for charts of dispersion curves clearly define the frequency, phase velocity, and wavenumber that can be found over a non-damaged body, so deviations from these charts indicate local structure failures.

3 Methodology

The theoretical analysis of wave action in circular tubes is not trivial. Moreover, and paradoxically, the modeling of guided waves in 1D structures such as rods is more complicated than that of structures with two infinite dimensions, like plates [7]. Therefore, this work is based on computational numerical analysis, using the methods presented in Sections 3.1 and 3.2.

3.1 Dispersion Curves

Generation of dispersion curves is carried out with the Semi-Analytical Finite Element Method (SAFE), proposed initially by Cegla [8] and extensively used by Groth [9], which used a circular waveguide with the same cross-section of interest here. In this case, if the symmetry radius is large enough, results quickly converge to those of a straight waveguide [7]. Method implementation is carried out through an axisymmetric model in the form of a ring, as shown in Figure 1a, where one specifies the number of wavelengths with which the structure is expected to vibrate.
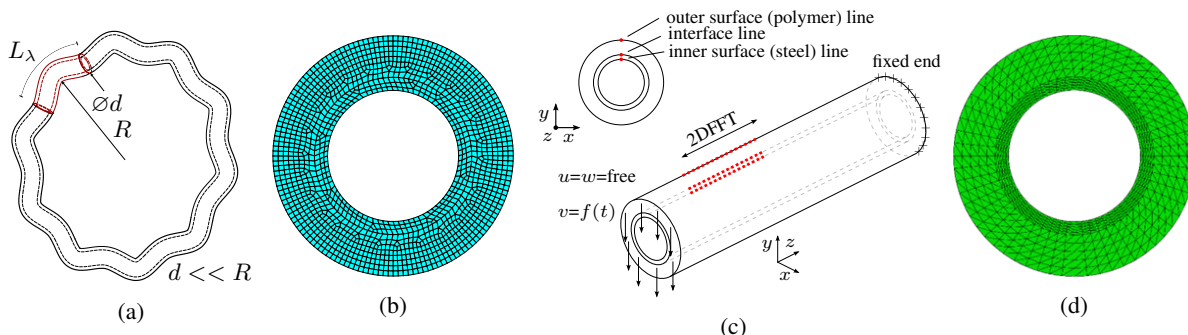

Figure 1. (a) Axi-symmetric model, (b) mesh of the axisymmetric model, (c) schematic of the explicit dynamics model with the excitation and representation of the nodes (red line) and contours, (d) mesh used in the explicit dynamics model.

The waveguide's cross-section is that of the ring, whose symmetry radius is much larger. A mesh with 3.00 mm bilinear quadrilateral elements was applied for the studied geometries, as can be seen in Figure 1b. Model simulation is made with the Ansys commercial finite-element package. An explicit dynamics model is also used as a validation reference. For this second method, the pipe is modeled in finite elements with a total length of 20.00 m (z-direction), and a prescribed displacement is applied on its front face while the back face is clamped (Figure 1c), generating a pure-bending configuration. Linear tetrahedral elements of 4 nodes are used, with a discretization of 25.00 mm in the outer layer, 16.00 mm in the interface, and 1.35 mm in the inner face, all along the z axis. Figure 1d shows the mesh used in the explicit model.

The double Fourier transform (2DFFT) is used to transform the temporal and spatial domain into the frequency domain. As recommended in Tormen Haan De Oliveira [10], the temporal response on the waveguide is collected along a sequence of equally spaced material points in the axial direction, resulting in a data matrix with dimensions of the number of points in time by the number of points in space. The double transform applied in this domain takes the response to the frequency versus wavenumber domain, allowing the data to be superimposed on the dispersion curves chart of the studied geometry, which shows on which modal waves the applied excitation travels. Data are collected along lines parallel to the pipe axis, on the outer surface (polymer), at the interface of the two media, and on the inner free surface (steel), as shown in Figure 1c.

3.2 Models analyzed

The analyses were performed on three different tube models, as depicted in Figure 2. Material properties and dimensions for each tube model are given in Table 1 and Table 2, respectively.
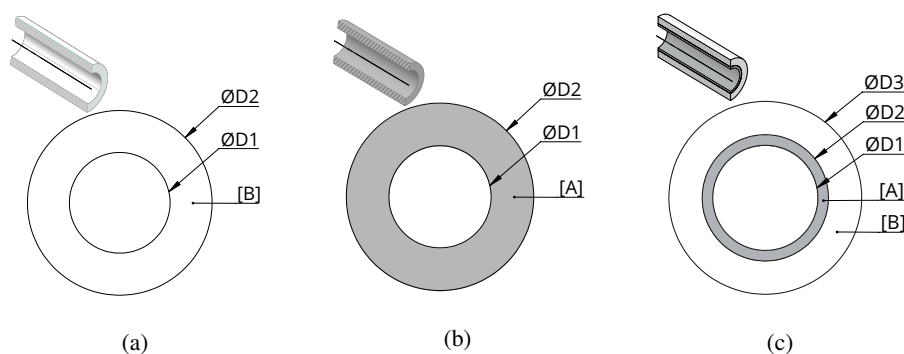

Figure 2. Tube models used in the study: (a) Polymer, (b) Steel, (c) Steel-Polymer.

Table 1. Tube materials and properties.

ID	Materials	E [GPa]	ρ [kg/m^3]	ν
[A]	Structural Steel	200.00	7860.00	0.30
[B]	Polymer	0.80	800.00	0.40

Table 2. Tube diameters.

Case	D_1 [mm]	D_2 [mm]	D_3 [mm]
Polymer	254.00	465.80	-
Steel	254.00	465.80	-
Steel-Polymer	254.00	305.00	465.80

4 Results

This chapter describes the results obtained from the dispersion curves of the three tubes analyzed, as well as the validation of the dispersion curves of the steel-polymer tube through an explicit dynamics scheme carried out in the commercial package Abaqus®/Explicit.

4.1 Analysis of dispersion curves for the different configurations studied

Using the axisymmetric method, dispersion curves were constructed for the configurations described in Figure 2. Results are presented both in the $f \times k$ and $v \times f$ domains for the three tube configurations. To decrease response complexity and to study each mode in greater detail, a narrow window of 0.00 kHz to 2.00 kHz, 0.00 rad/m to 6.00 rad/m and 0.00 km/s to 5.20 km/s is applied. Each curve is associated with a modal wave, that is, a mode of propagation. The modes of torsion, longitudinal, and bending are called fundamental modes and start from the origin of the $f \times k$ graphs, shown in Figure 1. Note in Figure 3 that there is a large number of modal waves outside the analyzed region. Lamb modes 1 and 2 are highly dispersive, which means that it is a composite excitation with
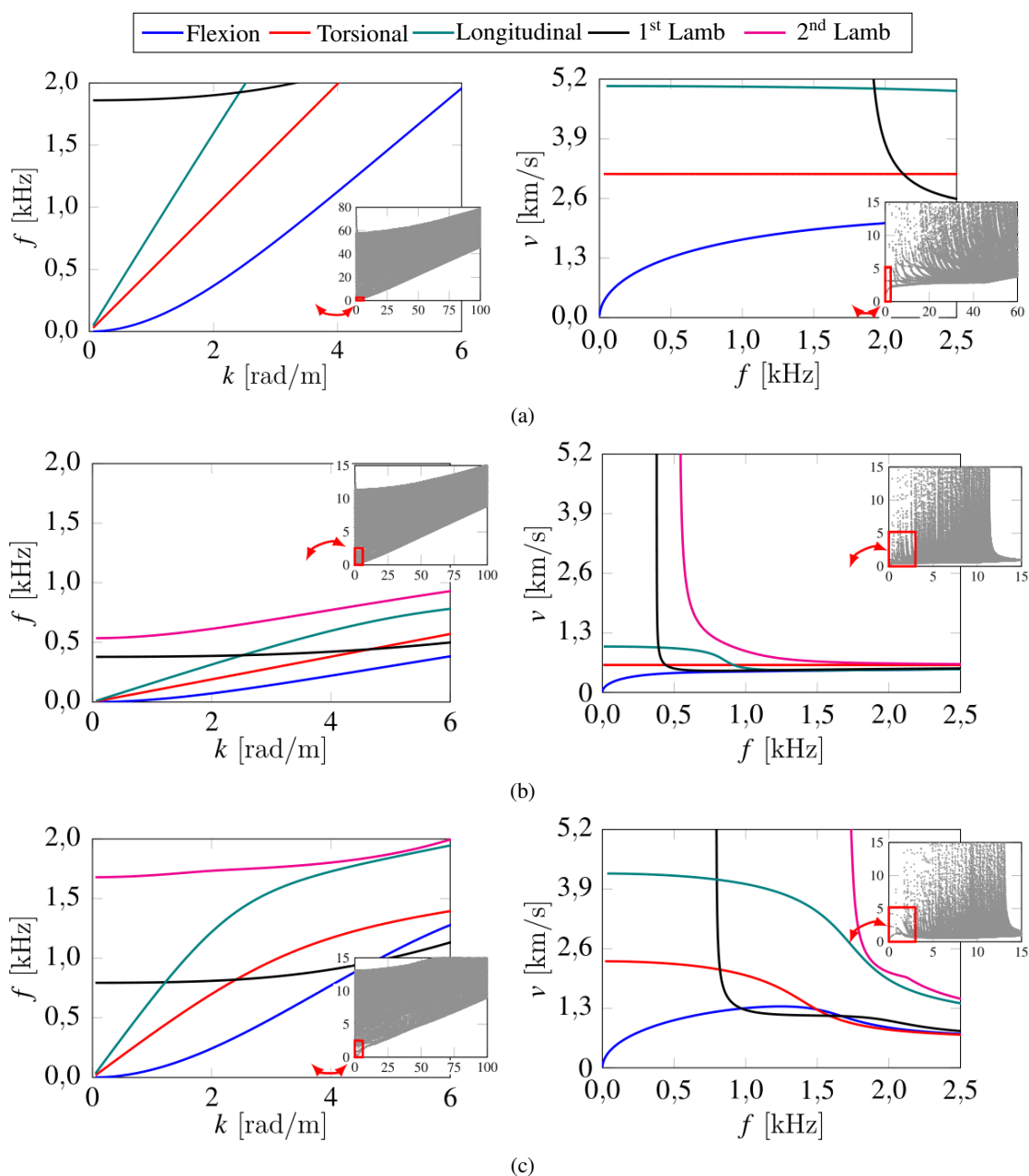

Figure 3. $f \times k$ and $v \times f$ for the cases Steel, Polymer and Steel-Polymer.

different frequencies. For steel and polymer, the velocity of the dispersion curves tends to be closer to the P-wave and S-wave in approximate form $v_p = \sqrt{E/\rho}$ and $v_s = \sqrt{G/\rho}$. One also observes that for high values of k, the bending modal wave and Lamb waves tend to travel at the speed of the Rayleigh wave. That is because, for high values of k (small wavelengths), these waves do not perceive the boundaries of the structure and interact only with the nearest free edge, concentrating more energy at the surface as a Rayleigh wave does.

4.2 Validation of Scatter Curves via Explicit Dynamics

This section describes the models simulated in the explicit dynamics scheme in the Abaqus®/Explicit software. The displacements are applied to the Steel-Polymer model in three distinct configurations referring to the modal forms of the pure bending mode. The function $f(t)$ characterizing the displacement fields is of the tone-burst type, expressed in eq. (3), where A_0 is the amplitude, f_0 the average frequency, and the number of cycles (n). The duration of excitation is related to the average frequency and the number of cycles in the form $t_d = n/f_0$. The excitation parameters in the different cases are outlined in Table 3.

$$f(t) = \frac{A_0}{2}\left(1 - \cos\left(\frac{2\pi f_0 t}{n}\right)\right)\sin\left(2\pi f_0 t\right) \tag{3}$$

Table 3. Excitation parameters of the cases studied in explicit dynamics.

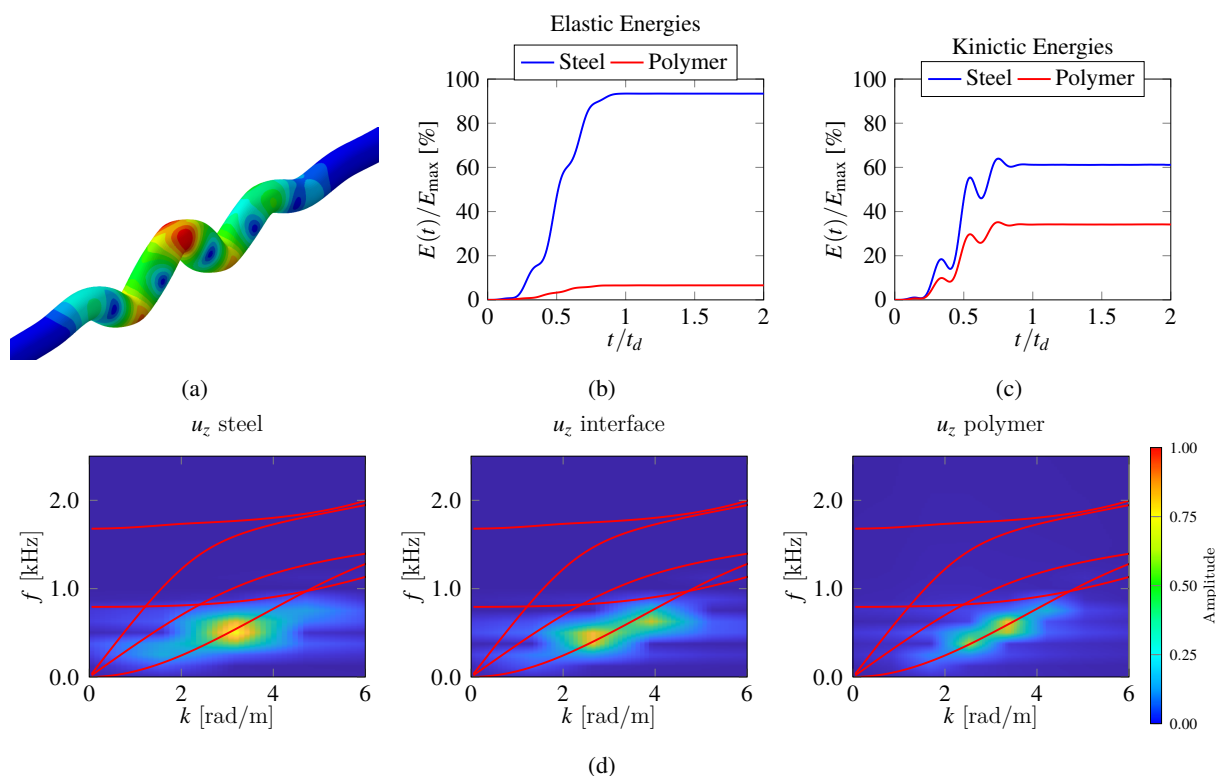| Case	f_0 [Hz]	n	A_0 [nm]	t_d [ms]
1	500.00	2.00	1	4.00
2	1000.00	2.00	1	2.00
3	1700.00	2.00	1	1.17

Figure 4. *Case 1*: (a) Three-dimensional model, (b) distribution of elastic energy, (c) distribution of kinetic energy in steel and polymer and (d) dispersion curves and displacement amplitude.
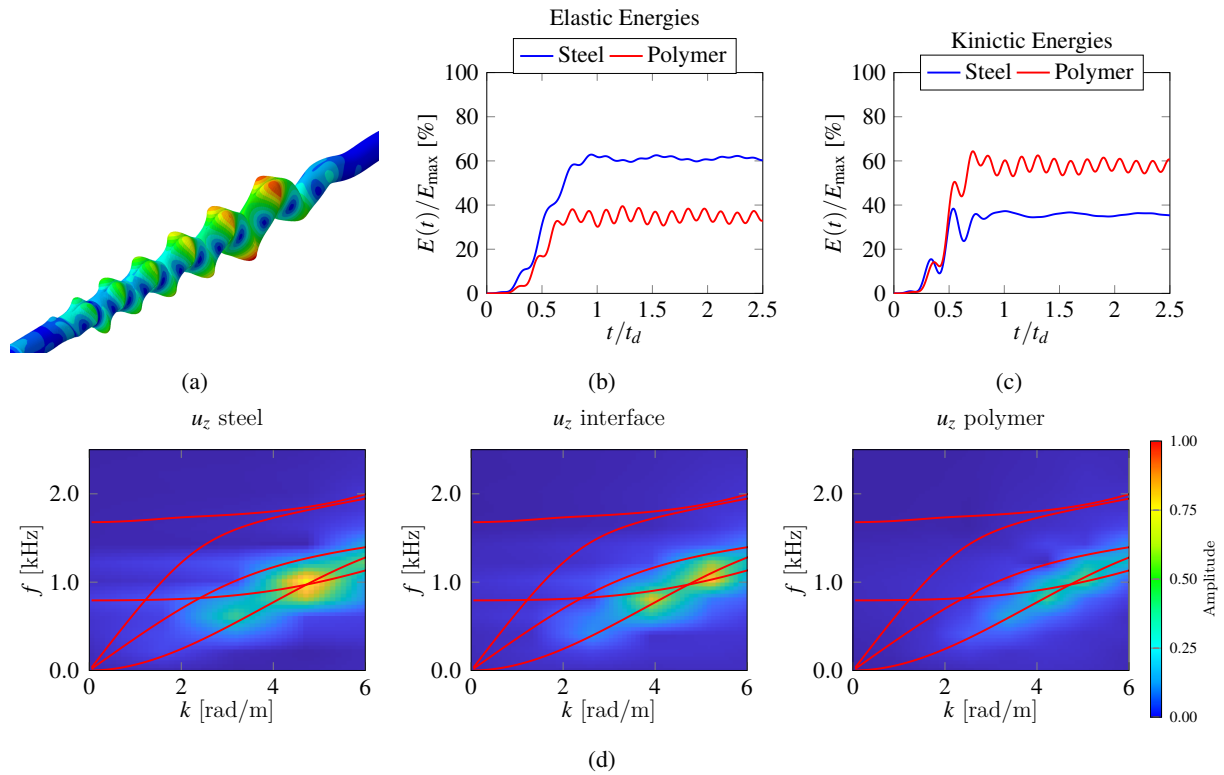
Figure 5. *Case 2*: (a) Three-dimensional model, (b) elastic energy distribution, (c) kinetic energy distribution in steel and polymer and (d) dispersion curves and displacement amplitude.
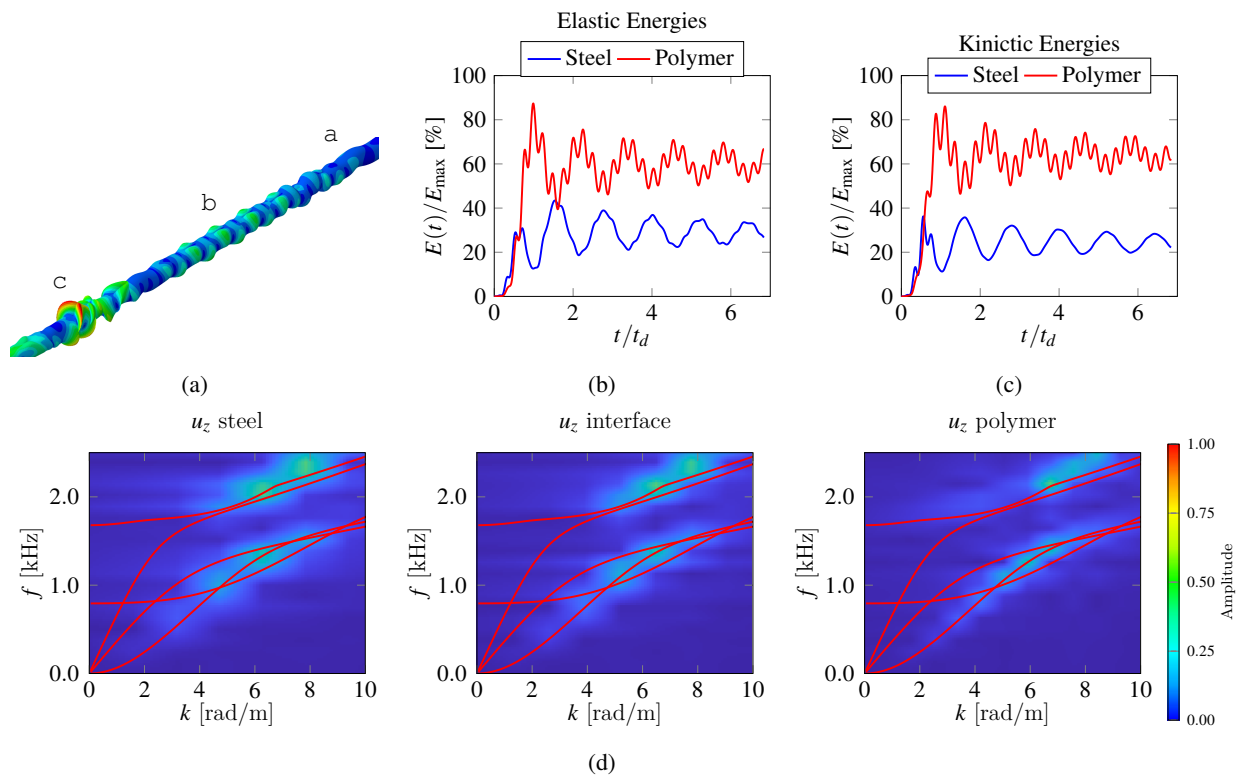

Figure 6. *Case 3*: (a) Three-dimensional model, (b) elastic energy distribution, (c) kinetic energy distribution in steel and polymer and (d) dispersion curves and displacement amplitude.

The energy balance and Fourier transform results for cases 1, 2, and 3 are shown in Figure 4, 5 and 6, respec-

tively. On notes that for cases 1 and 2 and excitation frequencies from 0.50 kHz to 1.00 kHz, the bending mode is the governing one, whereas in case 3, a significant contribution of Lamb modes causes most of the excitation energy to travel through the polymer, as highlighted in the first and second Lamb modes marked as b and c in Figure 6. According to this analysis, the amount of energy in the steel and polymer layers is directly dependent on the frequency and wavenumber of the excitation, where polymer and steel tend to resist together to the displacement fields generated for small values of k and f. This behavior is satisfactorily approximated by the beam theory [2] and is analogous to that of a composite beam, which is similar to a series association. Another interesting result is the asymptotic curves that always converge at the polymer's Rayleigh velocity for high k and f values, indicating that the polymer works as an energy attractor.

5 Conclusions

It can be concluded that the function of the polymer completely changes the elastodynamic response of the pure steel tube, where at small wavenumber values (large wavelength), the model acts in such a way that steel and polymer resist together to the fields. In contrast, the polymer's energy becomes more evident as the frequency and wavenumber increase, so that the polymer dominates the asymptotic behavior for $k \longrightarrow \infty$.

Authorship statement. The authors hereby confirm that they are the sole liable persons responsible for the authorship of this work, and that all material that has been herein included as part of the present paper is either the property (and authorship) of the authors, or has the permission of the owners to be included here.

References

[1] O. Vestrum, L. E. B. Dæhli, O. S. Hopperstad, and T. Børvik. Constitutive Modeling of a Graded Porous Polymer Based on X-Ray Computed Tomography. *Materials & Design*, vol. 188, pp. 108449, 2020.

[2] E. B. Groth, T. G. R. Clarke, Schumacher da G. Silva, I. Iturrioz, and G. Lacidogna. The Elastic Wave Propagation in Rectangular Waveguide Structure: Determination of Dispersion Curves and Their Application in Nondestructive Techniques. *Applied Sciences*, vol. 10, n. 12, pp. 4401, 2020.

[3] Y. Da, G. Dong, Y. Shang, B. Wang, D. Liu, and Z. Qian. Circumferential defect detection using ultrasonic guided waves: An efficient quantitative technique for pipeline inspection. *Engineering Computations*, vol. 37, n. 6, pp. 1923–1943, 2020.

[4] D. Hesse and P. Cawley. Surface wave modes in rails. *The Journal of the Acoustical Society of America*, vol. 120, n. 2, pp. 733–740, 2006.

[5] P. W. Loveday. Guided Wave Inspection and Monitoring of Railway Track. *Journal of Nondestructive Evaluation*, vol. 31, n. 4, pp. 303–309, 2012.

[6] J. L. Rose. *Ultrasonic Guided Waves in Solid Media*. Cambridge University Press, New York NY, 2014.

[7] P. Wilcox. Dispersion and excitability of guided acoustic waves in isotropic beams with arbitrary cross section. In *AIP Conference Proceedings*, volume 615, pp. 203–210, Brunswick, Maine (USA). AIP. ISSN: 0094243X, 2002.

[8] F. B. Cegla. Energy concentration at the center of large aspect ratio rectangular waveguides at high frequencies. *The Journal of the Acoustical Society of America*, vol. 123, n. 6, pp. 4218–4226, 2008.

[9] E. B. Groth. *Propagação De Ondas De Tensão Em Hastes Retangulares No Intervalo De Frequência De (0;100 [khz])*. Mestrado, UNIVERSIDADE FEDERAL DO RIO GRANDE DO SUL, Porto Alegre, 2016.

[10] H. Tormen Haan De Oliveira. *Projeto de um colar de ondas guiadas para aplicação em tubulação enterrada*. Mestrado, UNIVERSIDADE FEDERAL DO RIO GRANDE DO SUL, Porto Alegre, 2017.